Azhar Int J Pharm Med Sci 2024; Vol 4 (2):58-67.

Open Access

Print ISSN: 2735-4598
Online ISSN: 2735-4601

(Research Article.)

Novel 2-oxo-tetrahydropyrimidine derivatives as BRAFV600E inhibitors targeting melanoma: Design, synthesis and anticancer activity.

Eman A. A. Baumy[1], Hanan G. Abdulwahab [*1], Hend M.A. El-Sehrawi [1]

[1] *Pharmaceutical Medicinal Chemistry & Drug Design Department, Faculty of Pharmacy (Girls), Al-Azhar University, Cairo 11884, Egypt*

***** Correspondence: Hanangaber@azhar.edu.eg

Article history: **Received** 24-09- 2023 **Revised** 9-10-2023 **Accepted** 30-01-2024.

Abstract: Pyrimidine-based scaffolds have been shown to have anticancer effect and to suppress $BRAF^{V600E}$ kinase activity. Therefore, in this research, a new series of **2-oxo-tetrahydropyrimidine 2a-f** was synthesized. The structures of the newly synthesized compounds were validated using Fourier transform infrared (FT-IR), Proton nuclear magnetic resonance (^{1}HNMR), Carbon-13 nuclear magnetic resonance (^{13}CNMR), mass spectroscopy and elemental analysis. *In vitro* testing was performed on all derivatives against $BRAF^{V600E}$ enzyme, in comparison with Vemurafenib to determine their enzyme inhibitory activity. The results revealed that all derivatives inhibited $BRAF^{V600E}$ enzyme with variable values (IC_{50}= 0.53±0.023 - 5.717±0.242 µM)**.** Compound **2e** was the most potent among the series showing moderate activity (IC_{50}= 0.53±0.023 µM) relative to the reference drug (IC_{50}= 0.052±0.003 µM). Furthermore, compound **2e** was subjected to *in vitro* cytotoxicity study against melanoma cell **WM266.4.** The cytotoxic study indicated that compound **2e** has a reasonable anticancer activity (IC_{50}= 19.58±0.7 µM), relative to Vemurafenib (IC_{50}= 7.681±.0.3µM). Molecular docking analysis against $BRAF^{V600E}$ kinase proved excellent fitting inside the binding site. Compound **2e** could be identified as a promising candidate for further research.

Keywords: 2-oxo-tetrahydropyrimidine, melanoma, $BRAF^{V600E}$, cytotoxicity, docking.

1. INTRODUCTION

Finding new approaches to skin cancer treatment and prevention is essential, due to the rise in skin cancer cases worldwide[1,2]. The rising number of skin cancer cases seems to be related to skin excessive exposure to UV radiation because of ozone depletion[3,4].

The deadliest form of skin cancer is melanoma, it is characterized by melanocyte proliferation and melanin accumulation, resulting in pigmentation of the skin, discoloration, and tumor growth. Melanoma exhibits a high level of mutation, which has been associated with DNA damage caused by ultraviolet radiation and/or errors in DNA replication[5,6].

The progressive development of a malignant melanocytic lesion begins with a starting trigger mutation, this leads to normal melanocyte hyperplasia and formation of the nevi. Nevi transforms into intermediate lesions, which transform into *in situ* melanoma with a high mutation degree. Finally, primary melanoma progresses to the invasive stage and develops into malignant melanoma[7]. Melanoma treatment includes surgical removal of the tumor, immunotherapy, radiotherapy and chemotherapy. The surgical excision of lesions is effective in the treatment of melanoma in its early stages. On contrary, metastatic melanoma can be fatal, thus there is a significant demand for targeted therapy.[8].

The mitogen-activated protein kinase pathway (MAPK; RAS-RAF-MEK-ERK), which directs vital biological processes such as cell growth, differentiation and proliferation, is overexpressed in melanoma[9].

Cite this article: Baumy, E., Abdulwahab, H., El-Sehrawi, H., Novel 2-oxo-tetrahydropyrimidine derivatives as BRAFV600E inhibitors targeting melanoma: Design, synthesis and anticancer activity. Azhar International Journal of Pharmaceutical and Medical Sciences, 2024; 4 (2):58-67. doi.10.21608/AIJPMS.2024.238657.1237
DOI : 10.21608/AIJPMS.2024.238657.1237

Among the various mechanisms responsible for abnormal over expression of MAPK pathway signaling in melanoma is BRAF mutation that is the most frequent genetic abnormality detected in melanoma[10]. Among BRAF mutations, $BRAF^{V600E}$ was the most well-established one and it was discovered in approximately 50% of melanoma cells .This made $BRAF^{V600E}$ inhibitors one of the first choices for targeted melanoma therapy[11,12].

In recent years, diverse pharmacological effects of tetrahydropyrimidine compounds were reported such as anti-inflammatory, antiviral, calcium channel blocking, antibacterial, antifungal and anticancer properties[13]. Considering melanoma, drugs and lead compounds bearing the pyrimidine scaffold are proposed to be promising candidates, for their prospective cytotoxic properties, due to inhibition of BRAF. For example, **Dabrafenib (Taflinar ®)**, an FDA-approved drug for the treatment of tumors bearing mutant BRAF[14]. Another promising $BRAF^{V600E}$ inhibitor is, **Encorafenib** (**Braftovi ®**), the most recent FDA-approved drug directed for metastatic melanoma treatment [15]. In addition, **BI882370**, is an inhibitor that demonstrates a remarkable potency in inhibition of $BRAF^{V600E}$ kinase activity[16] (**Figure 1**).

On the other hand, sulfonamide moiety was found in several approved $BRAF^{V600E}$ targeted drugs, such as Dabrafenib**,** Encorafenib, and Vemurafenib (**Zelboraf ®**) (**Figure 1**). Moreover, sulfonamide moiety was also found in many ligands and investigated candidate as **BI882370**[16,17]. Furthermore, sulfonate moiety is a bioisostere of the sulfonamide one. They possess significant pharmacological applications in pharmaceutical research. Numerous reports have focused on the anticancer effects of the compounds with an aryl sulfonate moiety[18,19].

2. METHODS

2.1 Chemistry

In the **supplementary data**, all information regarding the chemicals and various analysis tools was provided. The staring aldehydes **1 a-c** were prepared according to the literature[20].

2.1.1 Synthesis of 2-oxo-tetrahydropyrimidine 2a-f.

A mixture of acetoacetanilde or ethylacetoacetate (5mmol), appropriate aldehyde **1a-c** (5mmol), urea (7.5mmol) and 5 drops of HCl was stirred at 100 ºC for 3 hrs. The formed solid mass was rinsed with water (to get rid of excess urea) and the product was crystallized from ethanol.

4-(6-methyl-2-oxo-5-(phenylcarbamoyl)-1,2,3,4-tetrahydropyrimidin-4-yl)phenyl benzenesulfonate (2a).

IR (KBr) (cm^{-1}): 3254 (NH), 1667 (br., C=O), 1371, 1179 (S=O); **^{1}H NMR** (DMSO-d_6) δ (ppm): 2.02 (s, 3H, CH_3), 5.36 (s, 1H, CH), 6.98 -7.83 (m, 15H, Ar-H, NH), 8.75 (s, 1H, NH, D_2O exchangeable), 9.53 (s, 1H, NH, D_2O exchangeable); **^{13}C NMR** (DMSO-d_6) δ (ppm): 17.06 (CH_3), 54.51 (CH), 105.01, 119.60, 120.01, 121.94, 122.07, 123.15, 124.08, 127.94, 128.08, 128.50, 128.76, 129.76, 129.88, 134.95, 135.07, 138.61, 139.10, 143.51, 148.02, 150.17 (aromatic Cs and C=C), 152.36, 165.14 (2 C=O); **MS *m/z* (%)**: 463.78 (M^+, 31.87), 307.52 (100.00).

4-(6-methyl-2-oxo-5-(phenylcarbamoyl)-1,2,3,4-tetrahydropyrimidin-4-yl)phenyl 4-chlorobenzenesulfonate (2b).

IR (KBr) (cm^{-1}): 3367 (NH), 1663 (br., C=O), 1374, 1178 (S=O); **^{1}H NMR** (DMSO-d_6) δ (ppm): 2.02 (s, 3H, CH_3), 5.30 (s, 1H, CH), 7.00 -7.82 (m, 14H, Ar-H, NH), 8.76 (s, 1H, NH, D_2O exchangeable), 9.55 (s, 1H, NH, D_2O exchangeable); **^{13}C NMR** (DMSO-d_6) δ (ppm): 17.16 (CH_3), 54.71 (CH), 105.20, 119.81, 122.11, 122.25, 122.78, 123.39, 128.21, 128.54, 128.68, 129.55, 130.09, 130.16, 130.25, 138.58, 139.14, 140.19, 143.73, 148.05 (aromatic Cs and C=C), 152.50, 165.34 (2 C=O); **MS *m/z* (%)**: 497.62 (M^+, 23.85), 327.91 (37.35), 330.0 (25.95), 89.85 (100.00).

4-(6-methyl-2-oxo-5-(phenylcarbamoyl)-1,2,3,4-tetrahydropyrimidin-4-yl)phenyl 4-methylbenzenesulfonate (2c).

IR (KBr) (cm^{-1}): 3361 (NH), 1667 (br., C=O), 1370, 1176 (S=O); **^{1}H NMR** (DMSO-d_6) δ (ppm): 2.21 (s, 3H, CH_3), 2.37 (s, 3H, SO_2-Ph-CH_3), 5.36 (s, 1H, CH), 6.96 - 7.68 (m, 14H, Ar-H, NH), 8.74 (s, 1H, NH, D_2O exchangeable), 9.53 (s, 1H, NH, D_2O exchangeable); **^{13}C NMR** (DMSO-d_6) δ (ppm): 17.08 (CH_3), 21.18 (SO_2-Ph-CH_3), 54.59 (CH), 105.12, 119.57, 119.67, 121.94, 122.13, 122.64, 123.21, 127.93, 128.14, 128.23, 128.40, 128.91, 129.98, 130.20, 131.38, 131.50, 138.50, 139.13, 143.45, 145.75, 148.12 (aromatic Cs and C=C), 152.40, 165.21 (2 C=O); **MS *m/z* (%)**: 477.69 (M^+, 27.67), 439.64 (100.00).

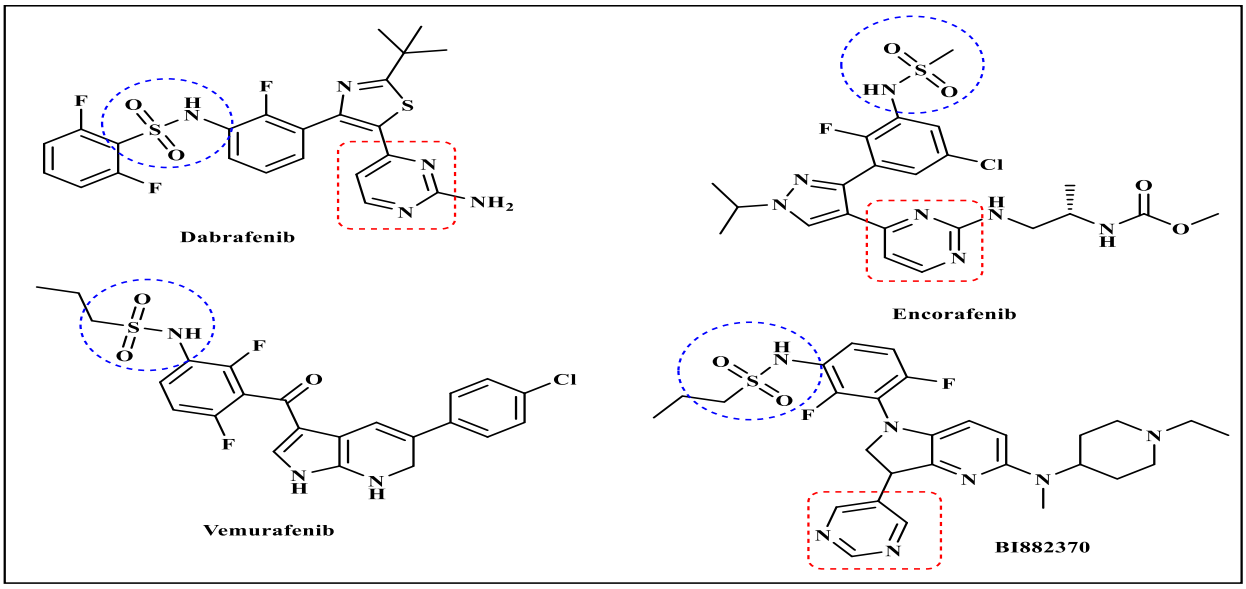

Figure 1. Some reported BRAF^{V600E} inhibitors that contain pyrimidine and sulfonamide moiety.

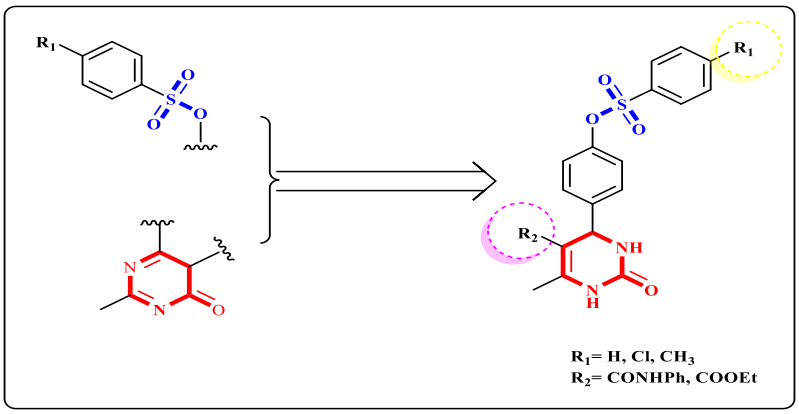

Figure 2: Design of 2-oxo-tetrahydropyrimidine compounds containing benzene sulfonate moiety as BRAF^{V600E} inhibitors **2a-f.**

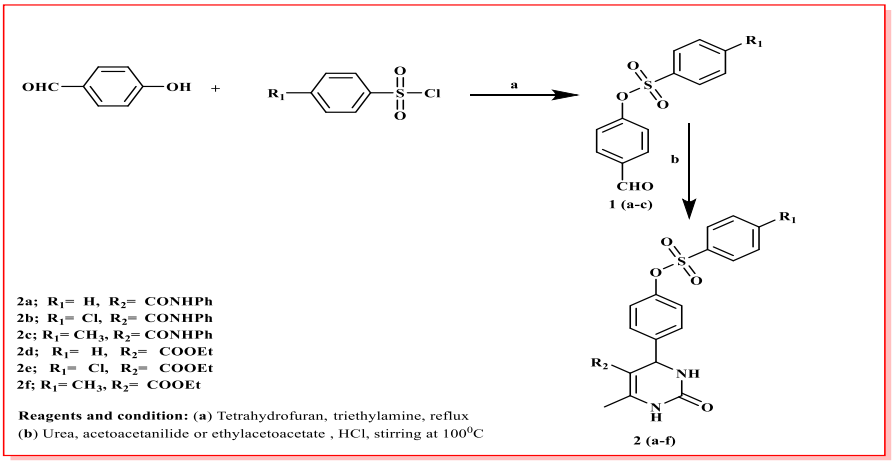

Scheme 1: The synthetic route of target compounds **2a-f**.

Table 1. Physical characters and elemental analysis of the new target compounds **2a-f**.

Comp.no.	Yield%	M.P. (ºC)	Mol. Formula (M. Wt)	Elemental analysis [%] Calcd. (Found)		
				C	H	N
2a	42	138 - 140	$C_{24}H_{21}N_3O_5S$ (463.51)	62.19 (62.26)	4.57 (4.61)	9.07 (9.01)
2b	35	118 -120	$C_{24}H_{20}ClN_3O_5S$ (497.95)	57.89 (57.95)	4.05 (4.10)	8.44 (8.48)
2c	30	128-130	$C_{25}H_{23}N_3O_5S$ (477.54)	62.88 (62.85)	4.85 (4.92)	8.80 (8.84)
2d	43	123- 125	$C_{20}H_{20}N_2O_6S$ (416.45)	57.68 (57.71)	4.84 (4.80)	6.73 (6.77)
2e	38	120- 122	$C_{20}H_{19}ClN_2O_6S$ (450.89)	53.28 (53.33)	4.25 (4. 21)	6.21 (6.15)
2f	35	148- 150	$C_{21}H_{22}N_2O_6S$ (430.48)	56.49 (56.57)	5.15 (5.18)	6.51 (6.55)

Table 2: IC_{50} of the tested compounds **2a-f** against $BRAF^{V600E}$ enzyme.

Comp. No.	Structure	$BRAF^{V600E}$ IC_{50} (µM)	Comp. No.	Structure	$BRAF^{V600E}$ IC_{50} (µM)
2a	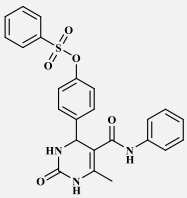	**1.581±0.067**	2e	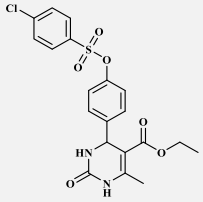	**0.531±0.023**
2b	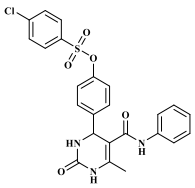	**5.717±0.242**	2f	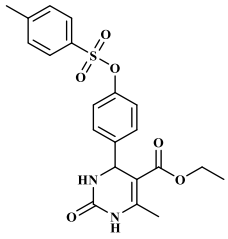	**0.779±0.033**
2c	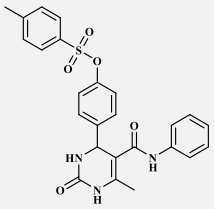	**1.547±0.066**	Vemurafenib	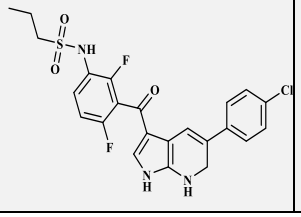	**0.052±0.003**
2d	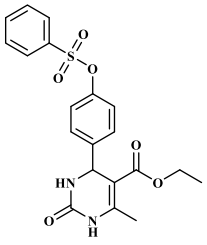	**2.149±0.091**			

Ethyl6-methyl-2-oxo-4-(4-((phenylsulfonyl)oxy)phenyl)-1,2,3,4-tetrahydropyrimidine-5-carboxylate (2d).

IR (KBr) (cm^{-1}): 3311 (NH), 1705, 1675 (C=O) 1374, 1183 (S=O); **^{1}H NMR** (DMSO-d_6) δ (ppm): 1.03 (t, 3H, $\underline{CH_3}$-CH_2 , *J*= 7.2 HZ), 2.23 (s, 3H, CH_3), 3.95(q, 2H, CH_3-$\underline{CH_2}$, *J*= 7.2 HZ), 5.11 (s, 1H, CH), 7.02 – 7.57 (m, 4H, Ar-H), 7.66 – 7.88 (m, 6H, Ar-H, NH), 9.22 (s, 1H, NH, D_2O exchangeable); **^{13}C NMR** (DMSO-d_6) δ (ppm): 14.01 ($\underline{CH_3}$-CH_2), 17.76 (CH_3), 53.49 (CH_3-$\underline{CH_2}$), 59.17 (CH), 98.71, 121.98, 127.97, 128.10, 128.15, 128.24, 129.68, 129.81, 134.05, 134.45, 135.00, 141.36, 147.95, 148.74 (aromatic Cs and C=C), 151.76, 165.12 (2 C=O); **MS *m/z* (%)**: 416.45 (M^+, 79.97), 293.23 (100.00).

Ethyl 4-(4-(((4-chlorophenyl)sulfonyl)oxy)phenyl)-6-methyl-2-oxo-1,2,3,4-tetrahydropyrimidine-5-carboxylate (2e).

IR (KBr) (cm^{-1}): 3399 (NH), 1682 (br., C=O), 1375, 1178 (S=O); **^{1}H NMR** (DMSO-d_6) δ (ppm): 0.98 (t, 3H, $\underline{CH_3}$-CH_2, *J*= 7.2 HZ), 2.21 (s, 3H, CH_3), 3.93 (q, 2H, CH_3-$\underline{CH_2}$, *J*= 7.2 HZ), 5.11 (s, 1H, CH), 6.99 (d, 2H, Ar-H, *J*= 8.8 HZ), 7.21 (d, 2H, Ar-H, *J*= 8.8 HZ), 7.69 (d, 2H, Ar-H), 7.84 - 7.86 (m, 3H, Ar-H, NH), 9.16 (s, 1H, NH, D_2O exchangeable); **^{13}C NMR** (DMSO-d_6) δ (ppm): 14.27 ($\underline{CH_3}$-CH_2), 18.06 (CH_3), 53.84 (CH_3-$\underline{CH_2}$), 59.68 (CH), 99.20, 122.35, 128.46, 130.36, 130.40, 133.44, 140.50, 144.53, 148.21, 149.06 (aromatic Cs and C=C), 152.22, 164.57 (2 C=O); **MS *m/z* (%)**: 450.19 (M^+, 16.01), 405.91 (52.24), 407.21(21.75), 354.94 (100.00).

Ethyl 6-methyl-2-oxo-4-(4-(tosyloxy)phenyl)-1,2,3,4-tetrahydropyrimidine-5-carboxylate (2f).

IR (KBr) (cm^{-1}): 3353 (NH), 1710, 1687 (C=O), 1376, 1171 (S=O); **^{1}H NMR** (DMSO-d_6) δ (ppm): 1.03 (t, 3H, $\underline{CH_3}$-CH_2, *J*= 6.8 HZ), 2.22 (s, 3H, CH_3), 2.40 (s, 3H, SO_2-Ph-CH_3), 3.90 (q, 2H, CH_3-$\underline{CH_2}$, *J*= 6.8 HZ), 5.11 (s, 1H, CH), 6.96 (d, 2H, Ar-H, *J*= 8 HZ), 7.25 (d, 2H, Ar-H), 7.44 (d, 2H, Ar-H, *J*= 8 HZ), 7.73 – 7.75 (m, 3H, Ar-H, NH), 9.20 (s, 1H, NH, D_2O exchangeable); **^{13}C NMR** (DMSO-d_6) δ (ppm): 14.06 ($\underline{CH_3}$-CH_2), 17.84 (CH_3), 21.25 (SO_2-Ph-CH_3), 53.59 (CH_3-$\underline{CH_2}$), 59.31 (CH), 98.87, 122.07, 128.05, 128.22, 130.32, 131.62, 144.12, 145.87, 148.12, 148.81 (aromatic Cs and C=C), 151.89, 165.39 (2 C=O); **MS *m/z* (%)**: 430.98 (M^+, 58.12), 94.05 (100.00).

2.2. *In vitro* BRAF^{V600E} inhibition assay:

Using Vemurafenib as a reference drug, the inhibitory activity of BRAF^{V600E} was assessed using a BRAF^{V600E} kinase assay kit. See the supplemental file for more information[21].

2.3 *In vitro* cytotoxic activity.

Utilizing MTT assay method[22], the *in vitro* cytotoxic activity of compound **2e** toward human melanoma cell line WM266.4 was evaluated as explained in **supplementary file**.

2.4 Docking.

The molecular docking simulation of the most potent compound **2e** was performed against BRAF^{V600E} (PDB ID: 3OG7) using MOE 14.0 software as outlined in **supplementary file**.

3. RESULT

3.1 Chemistry

In **scheme 1**, tetrahydropyrimidine derivatives **2a-f** were obtained with a yield of 30-43 %, by adopting the reported procedure[23]. Aldehydes **1a-c** were stirred with acetoacetanilide / ethylacetoacetate and urea in the presence of hydrochloric acid. The completion of the reaction was verified by TLC follow-up.

3.2 Biology

3.2.1 BRAF^{V600E} assay:

All the newly synthesized 2-oxo-tetrahydropyrimidine derivatives **2a-f** were assessed toward BRAF^{V600E} enzyme, compared to Vemurafenib (**Table 2**). All target compounds alleviated the enzyme activity in a moderate to weak manner showing IC_{50} values from 0.53 to 5.71 µM, compared to the reference drug Vemurafenib (IC_{50} = 0.052 ± 0.003 µM). Compound **2e** was the most potent among the series (IC_{50}= 0.52 ± 0.023 µM).

***3.2.2. In vitro* cytotoxic activity**: WM266.4 human melanoma cancer cells were used in the MTT assay to test the cytotoxic activity of compound **2e**, the most effective derivative against BRAF^{V600E} kinase. (**Table 3).**

3.3. Docking study

2-Oxo-tetrahydropyrimidine derivatives binding modes were investigated against **BRAF^{V600E}**. The co-crystallized ligand was employed as reference. The docking procedure was validated by re-docking the original ligand vemurafenib, generating RMSD value of 1.55 Å. The results of docking investigations revealed a good affinity of **2e** toward

the target enzyme compared to the reference molecule (**Table 4**).

Table 3. Cytotoxic activity of the most active compound **2e** against WM266.4 cell line.

Comp. No.	Structure	IC_{50} (μM)
2e	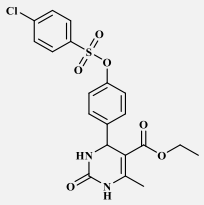	19.58±0.7
vemurafenib	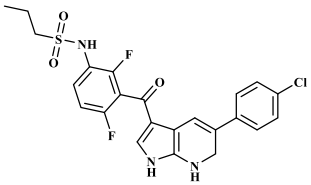	7.681±0.3

4. DISCUSSION

4.1 Chemistry

The chemical structure of the target compounds **2a-f** was ascertained through spectral data and elemental analyses. The ^{1}HNMR (DMSO-d6) spectra of compounds **2a-f**, displayed two characteristic singlets at a range of δ 2.02 – 2.23 and δ 5.11 – 5.36 ppm assigned to CH_3 and H6 protons of the tetrahydropyrimidine ring, respectively. Additionally, the ^{1}HNMR (DMSO-d6) spectrum of **2e**, showed the triplet - quartet pattern at δ .098, 3.85 ppm corresponding to ethyl ester protons, a singlet at δ 2.21 ppm attributed to tetrahydropyrimidine -CH_3 and a singlet at δ 5.11 ppm assigned to tetrahydropyrimidine-H_6. ^{13}CNMR spectrum of **2e** depicted signals at *δ* 14.27, *δ* 18.06, *δ* 53.84 and *δ* 59.68 ppm attributed to ethyl-CH_3, CH_3, CH_2 and CH, respectively. In addition to two characteristic signals at δ152.22 and 164.57 ppm assigned to 2 C=O. Finally, its **IR** spectrum showed strong absorption bands at 3399, 1682, 1375 and 1178 cm^{-1} ascertaining the presence of NH, C=O and S=O groups, respectively.

4.2 Biology

4.2.1. $BRAF^{V600E}$ inhibitory activity.

The main biological screening aimed to test the ability of the target compounds to inhibit $BRAF^{V600E}$ enzyme. IC_{50} values were determined for each compound, as mentioned in the results part. It was found that compounds having the ethyl ester moiety at tetrahydropyrimidine-C5, **2d-f** offered better enzyme inhibition (IC_{50}= 0.53 – 2.14 μM) than those containing phenyl carbamoyl one **2a-c** (IC_{50}= 1.54 – 5.71 μM). This finding was seen with derivatives, **2b**, **2c**, **2e** and **2f** that contain substituted benzene sulfonate moiety (R_1= Cl, CH_3). The contrary for the plain benzene sulfonate derivatives (R_1= H), the phenyl carbamoyl containing derivative **2a** has better activity than the ethyl ester containing one **2d**. Focusing on tetrahydropyrimidine derivatives with ester moiety, substitution of benzene ring with electron withdrawing chlorine atom (R_1= Cl) in **2e** or electron donating CH_3 (R_1= CH_3) in **2f** enhanced the activity compared to their unsubstituted analogue **2d.** On the other hand, regarding compounds containing the phenyl carbamoyl moiety, introduction of chlorine atom (R_1= Cl) in **2b** dropped the activity (about 4-fold), while substitution with the CH_3 group in **2c** doesn't have a significant effect, relative to **2a**, **(Figure 3).**

4.2.2. *In vitro* anticancer activity.

The most effective derivative against $BRAF^{V600E}$ kinase, **2e**, was chosen to test its cytotoxic activity against WM266.4 human melanoma cell line. **2e** showed moderate cytotoxic activity against the tested human melanoma cell WM266.4 (IC_{50} = 19.58±0.7μM), compared to Vemurafenib reference drug (IC_{50} = 7.68±0.3 μM).

4.3 Docking study.

In this study, the ligand Vemurafenib and the most potent compound **2e** were placed into the binding region of **$BRAF^{V600E}$** enzyme using the MOE-2014 program to perform a molecular docking simulation analysis. Vemurafenib was re-docked to confirm the docking procedure (**Figure 4**). The root-mean-squared-error (RMSD) was then calculated (1.55 A°), demonstrating that the docking technique used yielded accurate positions.

$BRAF^{V600E}$ X-ray structure bound to Vemurafenib (PDB; 3OG7) showed the important interactions of the ligand with the enzyme binding region .

The X-ray structure indicated that Vemurafenib binds to the kinase active site through the hinge region at the ATP-binding site in the cleft between the N and C lobes. The azaindole moiety forms two hydrogen bonds with the hinge residues, Cys532 and Gln530. The chlorophenyl moiety is oriented towards the solvent region, whereas the difluoro phenyl moiety is positioned in a hydrophobic pocket. Two H-bonds are formed between the sulfonamide group oxygens, Lys 483 and Gly 596 of the DFG sequence, as shown in **Figure 4**. Finally, the propyl

group is directed into the RAF selectivity pocket, which is a small pocket unique to the Raf family. Examining the docking results, compound **2e** showed promising affinity for BRAF^{V600E} and exhibited a preferred binding mode with docking score = 7.52 kcal/mol, compared to Vemurafenib, as proposed in **Figure 3**. The tetrahydropyrimidine core of **2e** occupies the adenine pocket, creating two hydrogen bonds with the hinge residues Gln530 and Cys532. Tetrahydropyrimidine moiety and its connected phenyl ring also formed hydrophobic interactions with key residues Val471, Ala 481, Thr529 and Trp531.

Furthermore, two oxygen atoms from the sulfonate moiety accepted two H-bonds from Asp594, the first residue in the DFG sequence, this interaction is thought to confer inhibitor specificity to the mutant kinase [24,25]. Furthermore, the 4-chloro-phenyl moiety was positioned in the RAF selectivity pocket, forming additional hydrophobic interactions with key residues Phe 468, Leu 514 and Phe 583. (**Figure 5**).

Table 4: The binding energies and interactions of compound **2e** and Vemurafenib in **BRAF^{V600E}** binding site.

Comp. no.	**Docking score (kcal/mol)**	**Amino acid residues (Bond length A^0)**	**Atom of compound**
2e	-7.52 kcal/mol	Gln 530 (2.89)	NH of pyrimidine ring
		Cys 532 (2.91)	NH of pyrimidine ring
		Asp594 (3.14)	O of sulfonate group
		Asp594 (2.53)	O of sulfonate group
Vemurafenib	-6.33 kcal/mol	Gln 530 (2.95)	NH of azaindole ring
		Cys 532 (3.02)	N of azaindole ring
		Lys 483 (3.77)	O of sulfonamide group
		Gly 596 (2.59)	O of sulfonamide group

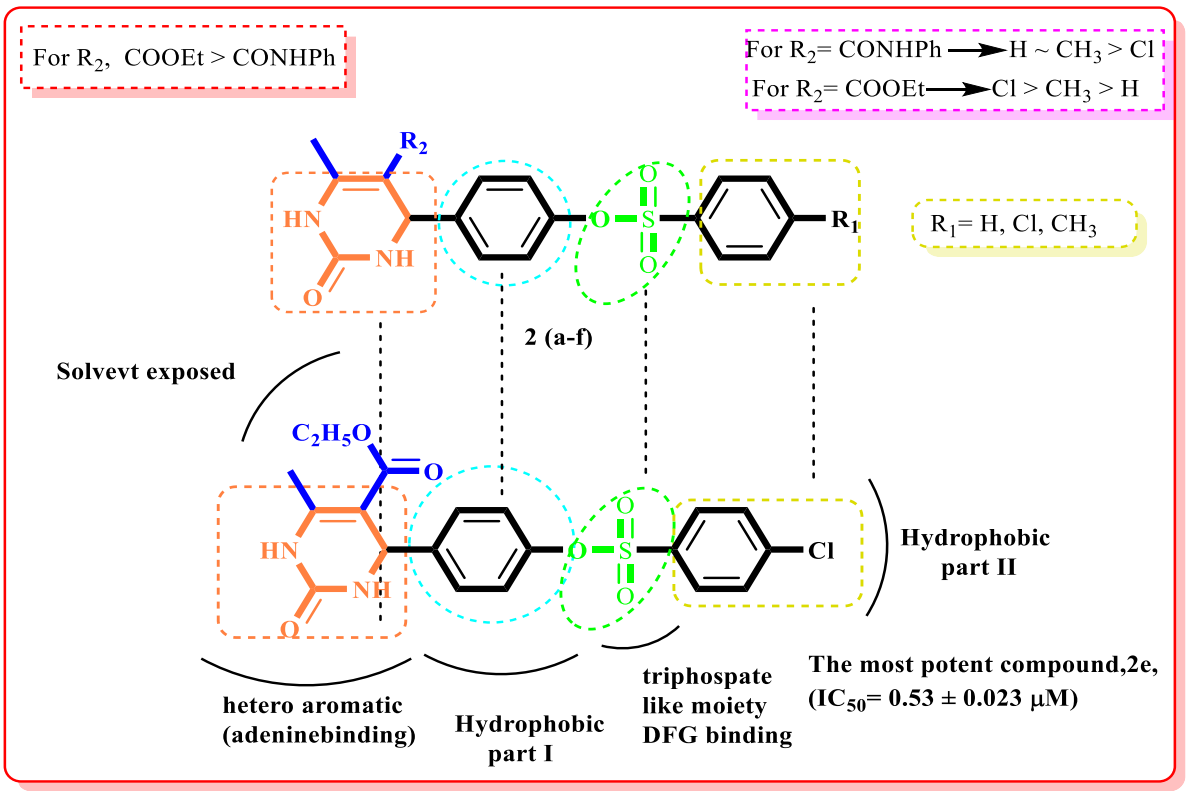

Figure 3. SAR and the proposed binding mode of the target compounds **2 a-f**.

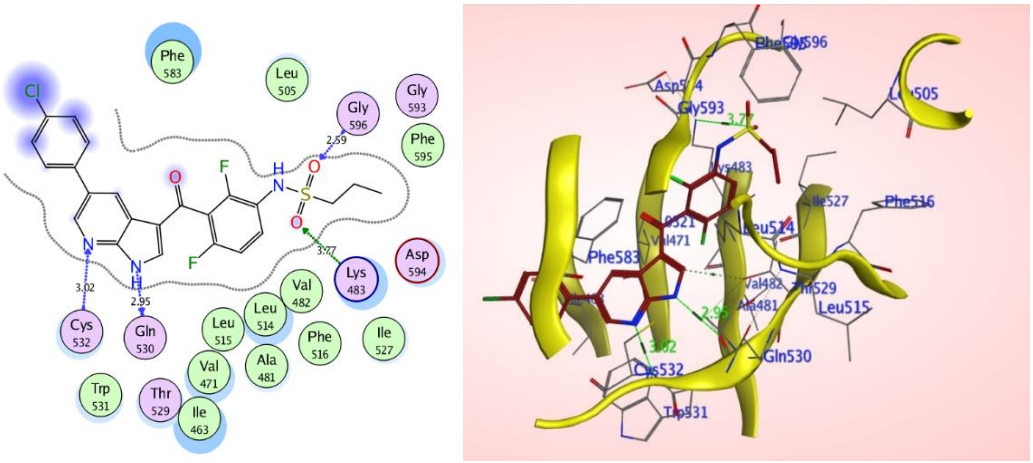

Figure 4. 2D and 3D binding mode of Vemurafenib docked into **BRAF^{V600E}** active site**.**

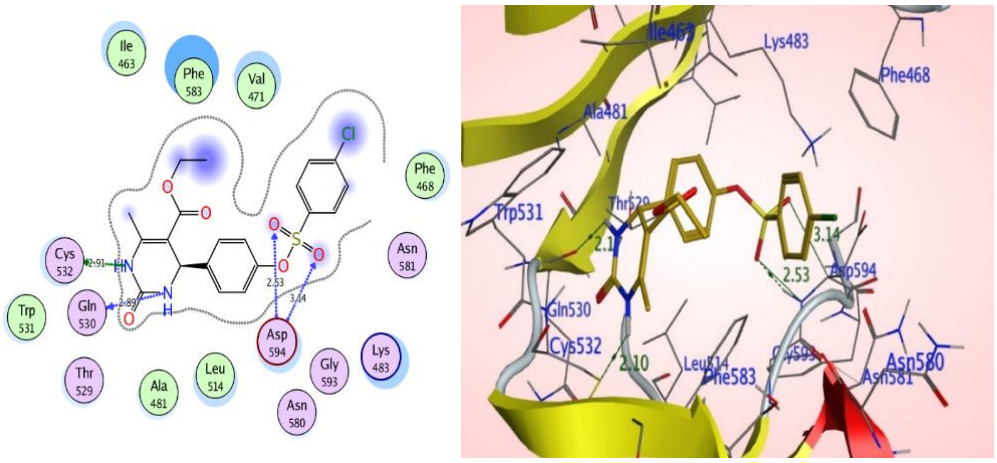

Figure 5. 2D and 3D binding mode of compound **2e** docked into **BRAF^{V600E}** active site**.**

5. Conclusions

Novel 2-oxo-tetrahydropyrimidine BRAF^{V600E} inhibitors were synthesized and evaluated as BRAF^{V600E} kinase inhibitors. The structures of the newly synthesized compounds were validated using IR, ^{1}HNMR, ^{13}CNMR, mass spectroscopy and elemental analysis. All derivatives inhibited BRAF^{V600E}, in enzyme assay and cytotoxicity tests against the WM266.4 cell line. Compound **2e** showed good inhibitory activity, compared to Vemurafenib. Molecular docking analysis showed that Compound **2e** fits well in the binding site of BRAF^{V600E} kinase, making it a promising candidate for further research.

Funding statement: No funding

Acknowledgments: None

Conflict of interest: The authors declare no conflict of interest.

Author's consent of publication: This paper is published under the full approval of authors.

Author Contribution: All authors had full access to all the information and took responsibility for data integrity and data analysis accuracy. Authors Eman A. A. Baumy, Hanan G. Abdulwahab, Hend M.A. El-Sehrawi designed the study. Author Eman A. A. Baumy performed the experimental work. Authors Eman A. A. Baumy, Hanan G. Abdulwahab wrote

the manuscript. Authors Hanan G. Abdulwahab, Hend M.A. El-Sehrawi supervised the work and revised the whole manuscript. The final manuscript was read and accepted by all the contributors**.**

List of Abbreviations:

RAF: Rapid activating fibrosarcoma

REFERENCES

1. Narayanan DL, Saladi RN, Fox JL. Ultraviolet radiation and skin cancer. Int J Dermatol. 2010;49(9):978-986. doi:10.1111/j.1365-4632.2010.04474.x

2. Khan NH, Mir M, Qian L, et al. Skin cancer biology and barriers to treatment: Recent applications of polymeric micro/nanostructures. J Adv Res. 2022;36:223-247. doi:10.1016/j.jare.2021.06.014

3. Norval M, Lucas RM, Cullen AP, et al. The human health effects of ozone depletion and interactions with climate change. Photochem Photobiol Sci. 2011;10(2):199-225. doi:10.1039/c0pp90044c

4. Umar SA, Tasduq SA. Ozone Layer Depletion and Emerging Public Health Concerns - An Update on Epidemiological Perspective of the Ambivalent Effects of Ultraviolet Radiation Exposure. Front Oncol. 2022;12(March):1-11. doi:10.3389/fonc.2022.866733

5. Saeed A, Ejaz SA, Khalid A, et al. Acetophenone-Based 3,4-Dihydropyrimidine-2(1H)-Thione as Potential Inhibitor of Tyrosinase and Ribonucleotide Reductase: Facile Synthesis, Crystal Structure, In-Vitro and In-Silico Investigations. Int J Mol Sci. 2022;23(21):13164. doi:10.3390/ijms232113164

6. Sample A, He Y ying. Mechanisms and prevention of UV-induced melanoma. Published online 2019:1-24. doi:10.1111/phpp.12329.Mechanisms

7. Eddy K, Shah R, Chen S. Decoding Melanoma Development and Progression : Identi fi cation of Therapeutic Vulnerabilities. 2021;10(February):1-13. doi:10.3389/fonc.2020.626129

8. Lacy KE, Karagiannis SN, Nestle FO. Advances in the treatment of melanoma. 2012;(January 2016). doi:10.7861/clinmedicine.12-2-168

9. Schummer P, Schilling B, Gesierich A. Long - Term Outcomes in BRAF - Mutated Melanoma Treated with Combined Targeted Therapy or Immune Checkpoint Blockade : Are We Approaching a True Cure ? Am J Clin Dermatol. 2020;21(4):493-504. doi:10.1007/s40257-020-00509-z

10. Sensi M, Nicolini G, Petti C, et al. Mutually exclusive NRAS Q61R and BRAF V600E mutations at the single-cell level in the same human melanoma. 2006; 61:3357-3364. doi:10.1038/sj.onc.1209379

11. Tanda ET, Vanni I, Boutros A, et al. Current State of Target Treatment in BRAF Mutated Melanoma. 2020;7(July). doi:10.3389/fmolb.2020.00154

12. Cheng L, Lopez-beltran A, Massari F, Maclennan GT, Montironi R. Molecular testing for BRAF mutations to inform melanoma treatment decisions : a move toward precision medicine. Nat Publ Gr. Published online 2017:1-15. doi:10.1038/modpathol.2017.104

13. Oliveira BGF, Daniel L, Modolo L V. MINI REVIEW A mini-review on Biginelli adducts with notable pharmacological properties ˆ ngelo de Fa. Published online 2015:363-373. doi:10.1016/j.jare.2014.10.006

14. Rheault TR, Stellwagen JC, Adjabeng GM, et al. Discovery of dabrafenib: A selective inhibitor of Raf Kinases with antitumor activity against B-Raf-driven tumors. ACS Med Chem Lett. 2013;4(3):358-362. doi:10.1021/ml4000063

15. Carr MJ, Sun J, Eroglu Z, Zager JS. An evaluation of encorafenib for the treatment of melanoma. Expert Opin Pharmacother. 2020;21(2):155-161. doi:10.1080/14656566.2019.1694664

16. Agianian B, Gavathiotis E. Current Insights of BRAF Inhibitors in Cancer. J Med Chem. 2018;61(14):5775-5793. doi:10.1021/acs.jmedchem.7b01306

17. Shahebaaz P, Rajesh P, Rajendra P, Chaskar MG, Rohidas A, Jaiprakash S. Bioorganic Chemistry Recent advances in B-RAF inhibitors as anticancer agents. 2022;120(December 2021).

18. Şenkardeş S, İhsan Han M, Gürboğa M, Özakpinar ÖB, Güniz Küçükgüzel. Synthesis and anticancer activity of novel hydrazone linkage-based aryl sulfonate derivatives as apoptosis inducers. Med Chem Res. 2022;31(2):368-379. doi:10.1007/s00044-021-02837-z

19. Khormi AY, Farghaly TA, Bayazeed A, Al-ghamdi YO, Abdulwahab HG, Shaaban MR. Novel thiazole derivatives incorporating phenyl sulphonyl moiety as potent BRAFV600E kinase inhibitors targeting melanoma †. Published online 2022:27355-27369. doi:10.1039/D2RA03624J

20. Tokalı FS, Demir Y, Demircioğlu İH, et al. Synthesis, biological evaluation, and in silico study of novel library sulfonates containing quinazolin-4(3H)-one derivatives as potential aldose reductase inhibitors. Drug Dev Res. 2022;83(3):586-604. doi:10.1002/ddr.21887

21. Obaid NM, Bedard K, Huang W yuarn. Strategies for Overcoming Resistance in Tumours Harboring BRAF Mutations. Published online 2017. doi:10.3390/ijms18030585

22. Mosmann T. Rapid Colorimetric Assay for Cellular Growth and Survival : Application to Proliferation and Cytotoxicity Assays. 1983;65:55-63.

23. Gülten Ş, Gezer U, Gündoğan EA. Fast and Efficient One-Pot Three-Component Synthesis of Some 1,2,3,4- Tetrahydro-6-methyl-N-phenyl-5-pyrimidinecarboxamide Derivatives via Biginelli Condensation Reaction. Lett Org Chem. 2019;17(5):366-371. doi:10.2174/1570178616666190819142221

24. Chessum N, Jones K, Pasqua E, Tucker M. Recent advances in cancer therapeutics. In: Progress in Medicinal Chemistry. Vol 54. Elsevier B.V.; 2015:1-63. doi:10.1016/bs.pmch.2014.11.002

25. Bollag G, Hirth P, Tsai J, et al. Clinical efficacy of a RAF inhibitor needs broad target blockade in BRAF-mutant melanoma. Nature. 2010;467(7315):596-599. doi:10.1038/nature09454